*Neuroscience* 346 (2017) 337–348

# LACTATE AND GLUTAMATE DYNAMICS DURING PROLONGED STIMULATION OF THE RAT BARREL CORTEX SUGGEST ADAPTATION OF CEREBRAL GLUCOSE AND OXYGEN METABOLISM

**SARAH SONNAY,** [a] **JOÃO M. N. DUARTE** [a] **AND NATHALIE JUST** [b*]

[a] *Laboratory for Functional and Metabolic Imaging, École Polytechnique Fédérale Lausanne, Switzerland*

[b] *CIBM-AIT core, Ecole Polytechnique Fédérale de Lausanne, Lausanne, Switzerland*

**Abstract—A better understanding of BOLD responses stems from a better characterization of the brain's ability to metabolize glucose and oxygen. Non-invasive techniques such as functional magnetic resonance spectroscopy (fMRS) have thus been developed allowing for the reproducible assessment of metabolic changes during barrel cortex (S1BF) activations in rats. The present study aimed at further exploring the role of neurotransmitters on local and temporal changes in vascular and metabolic function in S1BF. fMRS and fMRI data were acquired sequentially in α-chloralose anesthetized rats during 32-min rest and trigeminal nerve stimulation periods. During stimulation, concentrations of lactate (Lac) and glutamate (Glu) increased in S1BF by 0.23 ± 0.05 and 0.34 ± 0.05 μmol/g respectively in S1BF. Dynamic analysis of metabolite concentrations allowed estimating changes in cerebral metabolic rates of glucose ($\Delta CMR_{Glc}$) and oxygen ($\Delta CMR_{O2}$). Findings confirmed a prevalence of oxidative metabolism during prolonged S1BF activation. Habituation led to a significant BOLD magnitude decline as a function of time while both total $\Delta CMR_{Glc}$ and $\Delta CMR_{O2}$ remained constant revealing adaptation of glucose and oxygen metabolisms to support ongoing trigeminal nerve stimulation.** 

**Key words: fMRS, BOLD, barrel cortex, glutamate, ΔCMRGlc, lactate, adaptation.**

## INTRODUCTION

As $^{1}$H- and $^{13}$C-functional magnetic resonance spectroscopy (fMRS) studies develop both in humans and animals, the use of prolonged paradigms of stimulation is increasing (Mangia et al., 2007; Schaller et al., 2014; Just et al., 2013; Sonnay et al., 2015, 2016) and therefore an increased understanding of the mechanisms underlying these prolonged activations is needed. In particular, adaptation mechanisms cause weakened BOLD responses to repeated stimuli and involve several effects such as fatigue, tuning changes and altered response dynamics (reviewed in Larsson et al., 2015). Adaptation to repeated stimuli has been characterized at different stages along the whisker to barrel cortex pathway and encompasses several definitions from adaptation of sensory receptors to enhancement of inhibitory phenomena. However, adaptation is an inherent factor that also enables discrimination of subtle differences between subsequently presented stimuli (Maravall et al., 2007; Adibi et al., 2013; Musall et al., 2014). In fact, investigation of adaptation mechanisms has shown to be a great source of information on cortical processing. Many studies both in humans and in rodents used these nonlinearities to distinguish neuronal populations or designed protocols to minimize them (reviewed in Larsson et al., 2015). Adaptation/habituation effects have been included in early models of the hemodynamic response to brain activation (Aubert and Costalat, 2002; Buxton et al., 2004) using functions describing a sharp BOLD increase followed by a plateau after several seconds or minutes of stimulation. To our knowledge, only a few neuroimaging studies have addressed the effects of adaptation *per se* (Vafaee et al., 2012; Mintun et al., 2002; Lin et al., 2009; Moradi and Buxton, 2013). These studies considered its impact on $CMR_{O2}$ and CBF derived from PET or calibrated BOLD fMRI measurements since they may reflect changes in neurovascular coupling and suggested that investigating adaptation mechanisms during a prolonged stimulation process could be an interesting means of evaluating the balance between changes in CBF and changes in $CMR_{O2}$ (Moradi and Buxton, 2013; Larsson et al., 2015). Interestingly, adaptation can reflect changes in neurovascular coupling without changing BOLD responses or neuronal activity (Moradi and Buxton, 2013; Enager et al., 2009). These latter effects, if not taken into account, may lead to misleading interpretation of neuroimaging signals (Moradi and Buxton, 2013).

*Corresponding author. Address: Institut für Klinische Radiologie, Translational Research Imaging Center (TRIC), Albert-Schweitzer-Campus 1, Gebäude A16, Anfahrt: Waldeyerstr. 1, D-48149 Münster, Switzerland.

E-mail address: nathalie.just@ukmuenster.de (N. Just).

*Abbreviations:* fMRS, functional magnetic resonance spectroscopy; BOLD, Blood Oxygen Level Dependent; TGN, trigeminal nerve; S1BF, primary somatosensory barrel field cortex; Glu, glutamate concentration; GABA, γ-amminobutyric acid; Lac, lactate; Gln, glutamine; VOI, volume of interest; $\Delta CMR_{glc}$, change in cerebral metabolic rate of glucose; $\Delta CMR_{O2}$, change in cerebral metabolic rate of oxygen.

http://dx.doi.org/10.1016/j.neuroscience.2017.01.034

Studies of the rodent whisker to barrel cortex pathway showed that understanding of neurovascular mechanisms cannot be dissociated from understanding neurometabolic signals (Enager et al., 2009). $CMR_{O2}$ can be accurately measured using $^{13}C$-MR spectroscopy of glucose metabolism requiring robust protocols and measurement techniques (Sonnay et al., 2016; Hyder et al., 2001). Nevertheless, models of energy metabolism can also be used to infer $CMR_{O2}$ changes using $^{1}H$-MR spectroscopy measurements of Lactate and Glutamate (Schaller et al., 2014) although a number of oversimplifications exist and their impact on the results are debatable: in particular in this model, lactate was assumed to reflect non-oxidative metabolism only whereas it can also reflect oxidative metabolism (Attwell and Iadecola, 2002) or changes in oxidative metabolism that are neglected in the absence of glutamate variations. Moreover, the number of ATP molecules accounted for the process was decreased assuming that not all the glucose is transformed.

Recently, we demonstrated that $^{1}H$-fMRS studies could be translated to the rat barrel cortex (S1BF) during continuous prolonged activation (Just et al., 2013). Glutamate and lactate increased, as in human studies, further establishing these changes in metabolite concentrations as a hallmark of neuronal activity (Schaller et al., 2014).

In Just et al. (2013), continuous BOLD responses demonstrated strong habituation. We also measured prolonged BOLD responses to 2- hour forepaw stimulation in rats with a repeated 10sON-30sOFF-10sON paradigm of stimulation of the rat forepaw under α-chloralose anesthesia (Sonnay et al., 2015) and observed important BOLD baseline drifts that may be attributed to averaged local differences in $CMR_{O2}$, CBV and CBF across a large activated area. Habituation/adaptation phenomena in BOLD were minimized by switching stimulation frequencies between 2 and 3 Hz every 5 min. However, recent studies on adaptation demonstrated that BOLD responses do not accurately reflect adaptation processes (Buxton et al., 2014). Identical paradigms were used in a 13C-fMRS during infusion of glucose and 4-h forepaw stimulation of the rat forepaw (Sonnay et al., 2016). In these studies, we assumed that habituation effects had little impact on metabolic outcome.

The aim of this study was therefore to characterize and verify the presence and impact of habituation/adaptation processes determined with BOLD fMRI on the metabolic changes occurring during prolonged rat S1BF activation measured with an improved fMRS protocol including more rats and more averaging as well as a better positioning of the voxel of interest to avoid partial volume effects. Relative changes in $CMR_{O2}$ and $CMR_{Glc}$ were analyzed at 6.4 min after the start of a 32-min prolonged stimulation and after 12.8 min of prolonged stimulation to examine the effects of habituation.

## EXPERIMENTAL PROCEDURES

### Animals

All studies were performed following the approval of Service de la consommation et des affaires vétérinaires du canton de Vaud (Switzerland) and according to the federal guidelines of the Animal Care and approved by the local authority. Male Sprague–Dawley rats ($n$ = 23, 350 ± 40 g; Charles River, L'Arbresle, France) under isoflurane anesthesia (2–3%) vaporized in 30% $O_2$ in air were intubated, and mechanically ventilated. Two femoral arteries and one femoral vein were catheterized for blood gas sampling and blood pressure measurements as well as α-chloralose (an initial intravenous dose of 80 mg/kg was administered followed by a continuous intravenous infusion of 27 mg/kg/h at a rate of 2 ml/h) and pancuronium administrations. Respiration rate was monitored through a pillow (SA Instruments, Stony Brook, NY, USA) placed underneath each rat. Temperature was measured using a rectal sensor and regulated via control of the temperature of water flowing through tubing covering the body of each rat and linked to a temperature-regulated bain-marie. Less than 300 μl of arterial blood was sampled every 30 min and blood parameters directly measured using an AVL blood gas analyzer (Dotmed, USA). Mean Arterial blood pressure (MABP) was measured continuously using a transducer attached to the femoral artery catheter. Body temperature and blood parameters were maintained at physiological levels ($T$ = 37.5 °C ± 0.5 °C; pH = 7.4 ± 0.05, pCO2 = 39.7 ± 7 mmHg and MABP = 148.9 ± 11 mmHg) throughout each experiment. An intravenous femoral injection of Pancuronium Bromide (Sigma, Switzerland) of 0.7 ml per hour was performed to further minimize the remaining motion. Rats were positioned in a dedicated stereotactic holder equipped with ear and bite bars which was rotated in the magnet (30–45°) for a better positioning of voxels for fMRS over the barrel cortex and to avoid partial volume effects (Figs. 1 and 2).

### Trigeminal nerve stimulation (TGN)

Electrodes were percutaneously inserted in the left infraorbital nerve. Electrical stimulation of the left trigeminal nerve (TGN) was performed using an external stimulator (WPI, Stevenage, UK) as described in (Just et al., 2010). The paradigm of stimulation for fMRI was 60sOFF-60sON preceded by one minute and a half before the start of the paradigm and the paradigm of stimulation for fMRS was 60sON-60sOFF repeated for 32 min with pulse duration of 0.5 ms, stimulation frequency of 1 Hz and stimulation current amplitude of 2 mA.

### Magnetic resonance experiments

Experiments were performed on an actively shielded 9.4T/31 cm horizontal bore magnet (Magnex, Varian, Abingdon, UK) with 12-cm gradients (400mT in 120 μs) and an in-house made quadrature Transmit/Receive 20-mm surface coil. Shims were adjusted using FAST(EST)MAP (Gruetter and Tkác, 2000). fMRS was conducted first followed by BOLD fMRI in order to ensure that the metabolism was not perturbed by previous stimulation.

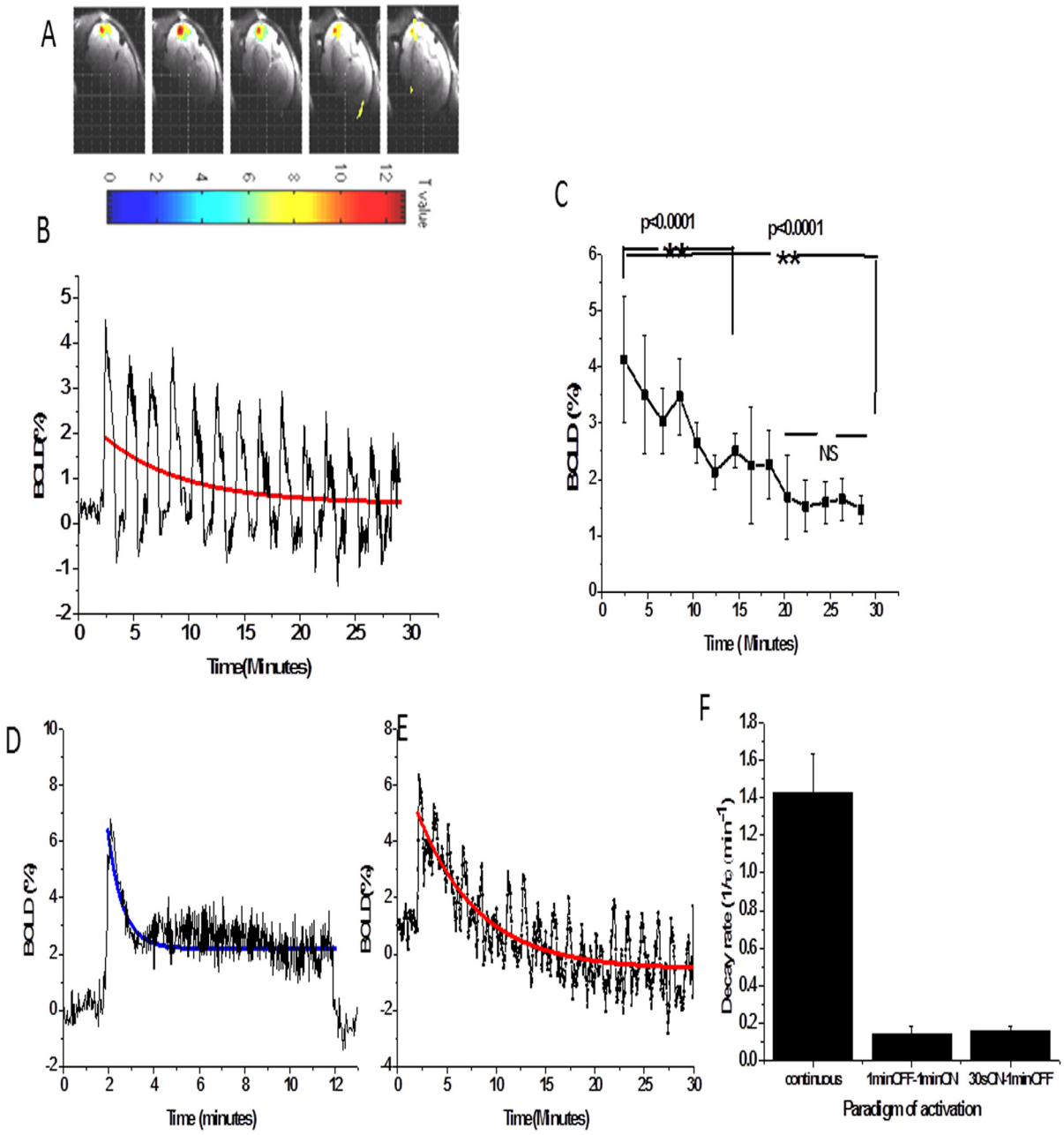


**Fig. 1.** (A) BOLD activation maps overlaid on Fast Spin-Echo images demonstrating focal activation in S1BF across several slices. EPI images during TGN stimulation were acquired after fMRS acquisitions in S1BF. (B) Average BOLD timecourse showing BOLD responses during application of a 1-min OFF-1minOn- paradigm of electrical trigeminal nerve stimulation repeated over 32 min. (C) Mean BOLD responses (averages at maximum peak height for each animal and across animals, Fig1.C) as a function of time during stimulation demonstrated a significant drop of BOLD magnitude 12 min after the start of stimulation ($\Delta$BOLD = 2.13% versus $\Delta$BOLD(t = 2.41minutes) = 4.13%, $p < 0.0001$, One-way repeated measures ANOVA + Bonferroni correction) and 28 min after the start of stimulation ($\Delta$BOLD = 1.47% versus $\Delta$BOLD (t = 2.41minutes) = 4.13%, $p < 0.0001$, One-way repeated measures ANOVA, + Bonferroni correction). There was no significant difference between BOLD responses at 20 and 28 min. (D, E) Continuous TGN stimulation used in (Just et al., 2013) and a 1 min OFF-30 s ON. . .paradigm repeated over 32 min used for previous test acquisitions of BOLD timecourses. The latter was strongly affected by Cerebral Blood Volume (CBV) changes as shown by important BOLD baseline drifts. Each BOLD timecourse was fitted to an exponential decay such that BOLD% = A.exp($-t/\tau$) + B where $1/\tau$ represented the decay rate of the BOLD responses per minute and was estimated using the fitting procedure. (F) Histogram comparing $1/\tau$ ($min^{-1}$) for each represented mean BOLD timecourse. Data are presented as Mean ± SEM.

### Proton fMRS

Localized Proton spectroscopy was performed using Spin Echo Full Intensity Acquired Localized Sequence (SPECIAL, TE = 2.8 ms, TR = 4 s) (Mlynarik et al., 2006). In the barrel cortex, the VOI size was $1.5 \times 3 \times 5$ $mm^3$ and was shimmed down to a linewidth of 10 ± 2 Hz. $^1$H spectra were acquired during 32-min of rest followed by 32 min of TGN stimulation corresponding to 480scans (30 × 16 FIDs) per period. The water sig-

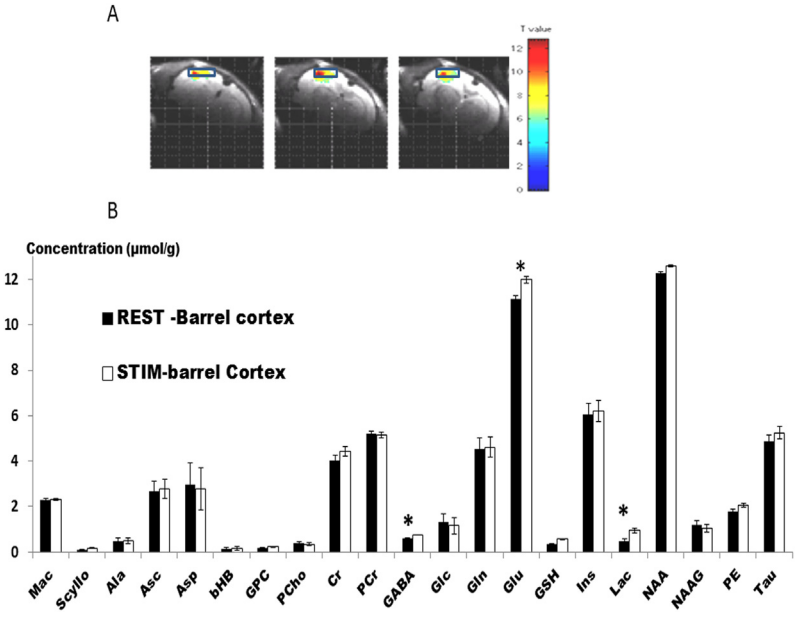


**Fig. 2.** (A) BOLD activation maps overlaid on Fast Spin-Echo images demonstrating focal activation in S1BF across several slices and voxel position for fMRS. The voxel of interest was positioned in order to cover the activated rat barrel cortex. Slices were chosen where BOLD maps had reproducibly demonstrated highest T-values (−4.16 mm to −1.40 mm from Bregma). (B) Neurochemical profile of S1BF during rest and TGN stimulation for 21 metabolites. Lac, Glu, GABA levels were significantly higher during stimulation ($p = 0.0015$, $p = 0.015$ and $p = 0.021$ respectively, one-way ANOVA and Bonferroni correction). Glc and Asp only demonstrated a tendency to decrease ($p > 0.05$). Mean ± SEM. Macromolecules: Mac; Scyllo-inositol: Scyllo; Ala: Alanine; Ascorbate: Asc; Aspartate: Asp; β-hydroxybutyrate: bHb; Glycerophosphocholine : GPC, Phosphocholine: PCho; Creatine: Cr; Phosphocreatine; γ-aminobutyric acid: GABA; Glucose: Glc; Glutamine: Gln; Glutamate: Glu; Glutathione: GSH; myo-inositol: Ins; Lactate: Lac; N-acetylaspartate: NAA; *N*-Acetylaspartylglutamic acid :NAAG; Phosphatidylethanolamines: PE; Taurine: Tau.

nal was suppressed using the VAPOR module containing a series of seven 25-ms asymmetric variable power RF pulses with optimized relaxation delays. To improve the signal localization, three modules of outer volume saturation (OVS) were interleaved with the water suppression pulses. The raw $^{1}$H-MRS spectra corrected for frequency drift and summed were used for LCModel analysis with a basis set of 21 simulated metabolites (Macromolecules: Mac; Scyllo-inositol: Scyllo; Ala: Alanine; Ascorbate: Asc; Aspartate: Asp; β-hydroxybutyrate: bHb; Glycerophosphocholine: GPC, Phosphocholine: PCho; Creatine: Cr; Phosphocreatine; γ-aminobutyric acid: GABA; Glucose: Glc; Glutamine: Gln; Glutamate: Glu; Glutathione: GSH; myo-inositol: Ins; Lactate: Lac; N-acetylaspartate: NAA; *N*-Acetylaspartylglutamic acid: NAAG; Phosphatidylethanolamines: PE; Taurine: Tau). Absolute metabolite concentrations were obtained using unsuppressed water signal as an internal reference. The Cramer–Rao lower bounds were used as a reliability measure of the metabolite concentration estimates.

The neurochemical profiles in S1BF were measured in 23 rats. S1BF spectra from one rat were discarded due to important lipid contamination. The signal-to-noise ratio (SNR) of spectra was calculated by measuring the intensity of the largest peak in the spectral range, N-Acetylaspartate (NAA) in this instance, and then measuring the noise intensity in the spectral range 0.0–0.5 ppm.

In order to validate neurochemical changes obtained in the rat barrel cortex upon barrel cortex activation, a BOLD free difference spectrum was calculated as described in (Just et al., 2013). After phasing and correction for $B_0$ shifts, 480 FIDs were summed per animal and then across 22 rats (1 rat demonstrated lipid contamination) for the 32-min rest period and for the 32-min stimulation period. Spectra were then subtracted from each other. In order to be able to quantify changes in metabolites due to stimulation, the $T2^{*}$ effect (or BOLD effect) responsible for a small decrease of the linewidth of the NAA peak and the tCr (Cr + PCr) peak needs to be removed. In order to proceed, a 0.3-Hz line broadening (lb) was applied to the NAA peak of the summed stimulated spectrum in order to match the linewidth of the summed rest spectrum. This was performed using an in-house written Matlab routine. The BOLD free difference spectrum obtained was then fitted using LCModel after simulation of a difference basis set containing positive lactate and glutamate changes and negative Aspartate and Glucose changes.

In S1BF, time courses of metabolites during rest and stimulation periods were also assessed with a temporal resolution of 6.4 min. The acquisition of 16 FIDs represented approximately 1 min. 30 times 16 FIDs were acquired in total during rest and stimulation periods. In order to obtain 5 rest spectra and 5 stimulation spectra per animal, metabolite time courses were obtained by averaging the first 96 FIDs (6 × 16 FIDs), then the next 96 FIDs (12 × 16 FIDs) etc... per animal during rest and stimulation periods. Spectra were then averaged per time point across the population of animals. Averaged spectra per time point during either rest or stimulation were fitted with LCModel. In the text, time points at 6.4 and 12.8 min corresponding to 6 min and 24 s (6 × 16 FID) and 12 min and 48 s (12 × 16 FIDs) respectively were essentially discussed.

## BOLD fMRI

First- and second-order shims were adjusted using FAST (EST)MAP (Gruetter and Tkác, 2000) resulting in water linewidths of 12 ± 2 Hz in a 216-µl (6 × 8 × 4.5mm$^3$) volume of interest positioned over fast-spin echo images acquired prior to EPI images. After echo re-alignment using a reference scan, BOLD responses were measured using single shot gradient echo EPI (TR/TE = 2500–2000/25 ms; FOV = 20x20 mm; matrix = 64 × 4; slice thickness = 1 mm; 8 slices, Bandwidth = 325 kHz, 900 volumes). Pre-processed images were analyzed with SPM8 (Matlab; The Mathworks; Natick, USA; Statistical Parametric Mapping, www.fil.ion.ucl.ac.uk/spm/) using the general Linear model (GLM) analyzing each voxel

independently and creating a parametric map of statistical significance (Friston et al., 1995). Within each analysis, the mean global intensities were mean scaled to an arbitrary value. Gradient Echo Echo Planar Imaging (GRE-EPI) time series were realigned, motion corrected and spatially smoothed with a 3D Gaussian kernel ($0.6 \times 0.6 \times 1\ mm^3$). The design model tested was a comparison between 'off' and 'on' conditions within each TGN stimulation paradigm. The paradigm was convolved with SPM's hemodynamic response function defined as a gamma-variate function and high-pass filtered. Residuals for the realigned rat movement were taken into account by submitting the realignment parameters (translations and rotations) as regressors. T-maps were calculated on a pixel by pixel basis. Thresholding criteria of 5 adjacent voxels, each with a Tscore > 3.0 were used to identify regions of interest. Only clusters comprising at least 5 pixels were considered significant ($p < 0.0001$ (corrected for multiple comparisons)). T-maps were overlaid on single shot gradient echo EPI images.

### Evaluation of changes in consumption rates of glucose ($\Delta CMR_{Glc}$) and oxygenation ($\Delta CMR_{O2}$)

Steady state levels of lactate and glutamate occur around 1.5 min after the onset of stimulation (Just et al., 2013). Therefore using similar assumptions as in Schaller et al. (2014), changes in glucose and oxygen metabolism can be inferred from the initial rise in lactate and glutamate. Here, rates of lactate and glutamate were estimated using either lactate evolution as a function of time resulting from averaging FIDs over time, per period (rest or stimulation), per animal and across animals every 6.4 min (96 FIDs).

Briefly and as explained in Schaller et al. (2014), steady-state levels of lactate and glutamate are reached approximately 1.5 to 2 min after the onset of stimulation resulting in a net increase of carbon tissue. The rate of lactate increase was thus calculated in μmol/g/min and then corresponded to non-oxidative glucose consumption, $\Delta CMR_{Glc,non\text{-}ox}$ as a result of glycolysis. The Glutamate rate of increase was also calculated in μmol/g/min as a result of the increase flux through pyruvate decarboxylase (PC) implying an oxidative glucose consumption, $\Delta CMR_{Glc,ox}$ (Schaller et al., 2014 and references therein; refer to Fig. 4A and B in Schaller et al. (2014) illustrating changes in glucose consumption associated with observed metabolite changes of Lac and Glu occurring during neuronal barrel cortex activation. It is assumed here that Lactate is generated by anaerobic glycolysis whereas glutamate changes are achieved through pyruvate carboxylation (PC).) The total rate of glucose consumption is the sum of non-oxidative and oxidative glucose consumptions.

Non-oxidative glucose consumption ($\Delta CMR_{Glc,non\text{-}ox}$) from lactate temporal evolution, oxidative glucose consumption ($\Delta CMR_{Glc,ox}$) from glutamate temporal evolution and their sum ($\Delta CMR_{Glc,tot}$) were evaluated at the start of stimulation assuming steady-states were reached after two minutes of stimulation. The relative increase of $\Delta CMR_{O2}$ during S1BF activation was calculated using the assumption that synthesis of glutamate from glucose produces 8ATPs out of 36 for complete oxidation of glucose and was calculate using: $\Delta CMR_{O2} = 5.5 \times \Delta CMR_{Glc,ox} \times 8/36$ (Schaller et al., 2014). In the latter, the contribution of the ATP production coupled to mitochondrial oxidation relative to the glucose used for glutamate synthesis was used as described by Schaller et al. (2014). It was also assumed that not all the glucose entering the TCA cycle from pyruvate was completely oxidized. Since newer steady states were obtained during prolonged S1BF stimulations, it was assumed that the same modeling process could be used to evaluate changes in the consumption rates of glucose and oxygen during habituation. Indeed, most of the considerations discussed in Schaller et al. (2014) regarding the assumptions made, hold here and must be carefully weighed against more accurate estimates using $^{13}C$ NMR Spectroscopy.

In the following and in order to better explore the effects of changes in Lactate and Glutamate as a function of time during prolonged stimulation on the calculation of $\Delta CMR_{Glc,non\text{-}ox}$, $\Delta CMR_{Glc,ox}$ and $\Delta CMR_{O2}$, three different methods were used. In Method1, Lactate and Glutamate changes due to stimulation were calculated relative to the rest period at each time point, in Method2 changes were considered during stimulation only and were therefore calculated relative to the previous point. Finally Method3 represents the calculation of $\Delta CMR_{Glc}$ from the Glc concentration measurements using fMRS.

### Statistics

Statistics were conducted using SPSS 22 (IBM SPSS Statistics, Germany). The Shapiro-wilk test in SPSS 22 was performed for all the variables demonstrating p values above 0.05 and therefore normality of each variable distribution. A one-way ANOVA test with Bonferroni correction was used to compare metabolite concentrations at rest and during stimulation. The significance level was set at 0.05. All the results are presented as Mean ± Standard error of the mean (SEM). An analysis of variance (ANOVA) with repeated measures was performed followed by Bonferroni-Holm corrections to compare time points for BOLD, Lac, Glu and $\Delta CMR_{Glc}$ and $\Delta CMR_{O2}$. The significance level was set at $p = 0.05$. All the results are presented as Mean ± Standard error of the mean (SEM) unless otherwise stated.

## RESULTS

### BOLD responses

Fig. 1 shows examples of BOLD timecourses obtained in S1BF upon prolonged TGN stimulations. Each of them demonstrated decreased BOLD amplitudes as a function of time attributed to habituation. TGN electrical stimulations using a 1minOFF-1minON... paradigm repeated over 32 min (Fig. 1A) led to a significant decrease of the BOLD response as shown in Fig. 1B, although habituation effects were visually considered mild compared to the continuous TGN stimulation used in (Just et al., 2013) and a 1 min OFF-30s ON...paradigm

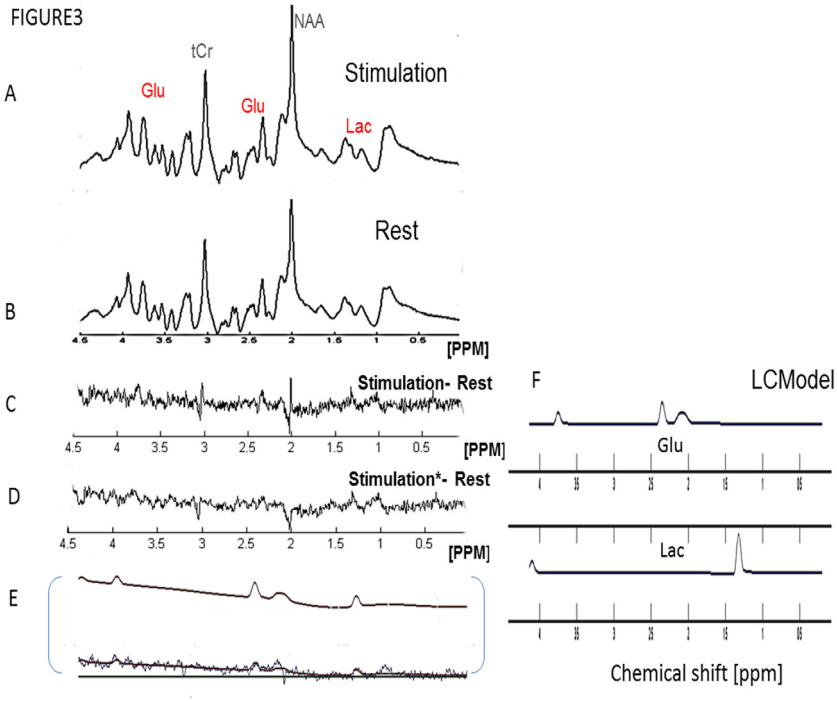


**Fig. 3.** BOLD free difference spectrum in S1BF and quantification of Lac and Glu. changes. (A) Summed stimulation spectra ($n$ = 22). (B) Summed rest spectra ($n$ = 22). (C) Difference spectrum between A and B before line-broadening of the group stimulation spectrum. (D) BOLD free difference spectrum after applying a 0.3-Hz line-broadening to the group stimulation spectrum showing positive lactate (1.32 ppm) and Glu peaks (2.38 ppm). A 0.3-Hz line broadening (lb) of the NAA peak was applied to the stimulation spectrum in order to match the linewidth of the rest spectrum. (E) LCModel fits to the entire BOLD-free difference spectrum and (F). Individual fits for Glutamate and Lactate. The BOLD free difference spectrum was fit with LCModel and a simulated basis set yielding positive quantitative changes for Glu and Lac (+0.34 ± 0.05 μmol/g and +0.23 ± 0.05 μmol/g, respectively.

repeated over 32 min as shown in Fig. 1**.E** and used for previous pilot acquisitions of BOLD timecourses. The latter was strongly affected by Cerebral Blood Volume (CBV) changes as shown by important BOLD baseline drifts while continuous stimulation did not allow acquisitions longer than 20 min as shown in (Just et al., 2013; Sonnay et al., 2015). Mean BOLD responses (averages at maximum peak height for each animal and across animals, Fig. 1**.C**) as a function of time during stimulation demonstrated a significant drop of BOLD magnitude 12 min after the start of stimulation (ΔBOLD = 2.13% versus ΔBOLD(t = 2.41minutes) = 4.13%, $p < 0.0001$, One-way repeated measures ANOVA + Bonferroni correction) and 28 min after the start of stimulation (ΔBOLD = 1.47% versus ΔBOLD (t = 2.41minutes) = 4.13%, $p < 0.0001$, One-way repeated measures ANOVA, Bonferroni corrected + Bonferroni correction). In order to characterize, the BOLD decay as a function of time, each BOLD timecourse was fitted to an exponential decay such that BOLD% = A.exp(−t/τ) + B where 1/τ represented the decay rate of the BOLD responses per minute and was estimated using the fitting procedure. Fig. 1F compares 1/τ for each represented mean BOLD timecourse. In order to validate τ as a measure of adaptation, the continuous BOLD timecourse measured over 10 min during TGN stimulation (Fig. 1D) and presented in (Just et al., 2013) was also fitted to an exponential decay and demonstrated a decay rate significantly faster (1.43 ± 0.2 $min^{-1}$) compared to the repeated paradigms (Fig. 1F) for which decay rates were in the same range (0,15–0.16 ± 0.04 $min^{-1}$).

### fMRS of the barrel cortex

High spectra SNR levels were reproducibly measured in S1BF (91 ± 8). LCModel was used for the quantification of 21 metabolites. Higher concentration metabolites (Glu, NAA, Ins, Tau, PCr, Cr) with Cramer-Rao lower bounds (CRLB) under 10% were considered to be reliably quantified whereas for all the other metabolites and especially Glc, GABA, Lac and Asp CRLB under 30% were considered acceptable and were kept for further analysis (Schaller et al., 2014). In the barrel cortex, lactate concentrations ranged between 0.43 and 0.5 μmol/g under rest conditions. Lac, Glu and GABA levels were significantly higher during stimulation ($p = 0.0015$, $p = 0.015$ and $p = 0.021$ respectively, one-way ANOVA and Bonferroni correction). Glc and Asp did not demonstrate significant changes ($p > 0.05$) (Fig. 2).

Within S1BF, the group BOLD-free difference spectrum between rest and stimulation using data from 22 rats confirmed these findings (Fig. 3). 32-min spectra were averaged across all animals during rest (Fig. 3A) and stimulation periods (Fig. 3B). The two spectra were then subtracted to obtain a difference spectrum (Fig. 3C). A 0.3-Hz line broadening was applied so that the linewidth of the stimulation spectrum matched the linewidth of the rest spectrum (Fig. 3D). The BOLD- free difference spectrum clearly shows positive peaks at 1.33 ppm for Lac and at 2.13 and 2.35 ppm for Glu (Fig. 3E, F). This BOLD free difference spectrum was fitted with LCModel (Fig. 3E, F) and a simulated basis set yielding positive quantitative changes for Glu and Lac (+0.34 ± 0.05 μmol/g and +0.23 ± 0.05 μmol/g, respectively).

### Temporal assessment of barrel cortex metabolic activity

Quantified metabolites with CRLB < 30% were plotted individually as a function of time as shown in Fig. 4. [Lac] increased 6.4 min after onset of stimulation (+152%, +0.77 μmol/g) followed by a new steady state at 0.74 ± 0.05 μmol/g lasting until the end of stimulation (Fig. 4A). Compared to the rest period, average lactate levels at 6.4 min were significantly higher during barrel cortex activation compared to 6.4 min at rest ($p < 0.05$, repeated measures ANOVA). Changes in lactate were

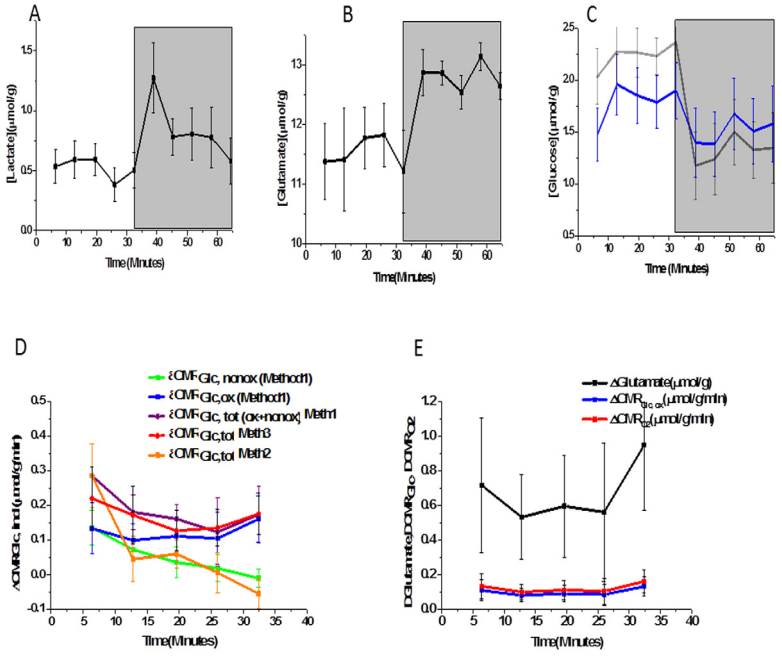


**Fig. 4.** (A) Timecourse of Lactate during 32 min of rest and 32 min of TGN stimulation (Gray shaded area). [Lac] increased 6.4 min after onset of stimulation ( + 152%; + 0.77 μmol/g) followed by a new steady state at 0.74 ± 0.05 μmol/g lasting until the end of stimulation. (B) Timecourse of Glutamate during 32 min of rest and 32 min of TGN stimulation (Gray shaded area). Glu levels were increased 6.4 min after onset of stimulation (+14.8%, $p < 0.01$) and remained stable (12.8 ± 0.2 μmol/g) until the end of stimulation. **C.** Timecourse of Glucose during 32 min of rest and 32 min of TGN stimulation (Gray shaded area). Significant decrease of Glc levels ($p = 0.03$) during stimulation was found (Gray timecourse) when excluding two individual timecourses showing no decreased Glc Levels. For consistency across metabolites, all timecourses were included (Blue timecourse). (D) Comparison of changes in metabolic consumption rates of Glucose ($\Delta CMR_{Glc,non\text{-}ox}$, $\Delta CMR_{Glc,ox}$ and $\Delta CMR_{Glc,\ tot}$) calculated from Lac and Glu changes as a function of time and using different methods based on the simplified model by Schaller et al. (2014). **In Method1**, changes in Lactate and Glutamate as a function of time were calculated as the difference between Lactate or Glutamate concentrations during stimulation and rest at their respective time point. In **Method2**, changes in Lactate and Glutamate as a function of time were calculated as the difference between Lactate or Glutamate concentrations at a specific time point relative to Lactate or Glutamate concentrations at the previous time point. **Method3** represents the calculation of $\Delta CMR_{Glc,\ tot}$ from glucose measurements (Fig. 4.C). Data were averaged across the population of rats and are presented as Mean ± SEM. Using Method1 for calculation, $\Delta CMR_{Glc,non\text{-}ox}$ (Green curve) dropped from 0.1 ± 0.01 μmol/g/min at the start of stimulation to 0.048 ± 0.002 μmol/g/min 19.2 min after the start of stimulation whereas $\Delta CMR_{Glc,ox}$ (Blue curve) remained stable. The sum of both curves allowed to evaluate $\Delta CMR_{Glc,tot}$ (Purple curve) largely influenced by non-oxidative metabolism. $\Delta CMR_{Glc,tot}$ evaluated using method1 was compared to $\Delta CMR_{Glc,tot}$ evaluated with Method2 (Orange curve) and Method3(Red curve), the latter demonstrating agreement with results observed with Method1. (E) Since $\Delta CMR_{Glc,ox}$ and $\Delta CMR_{O2}$ calculations were proportional to ΔGlu, their evolution as a function of time demonstrated identical patterns with $\Delta CMR_{Glc,ox}$ = 0.11 ± 0.06 μmol/g/min and $\Delta CMR_{O2}$ = 0.13 ± 0.07 μmol/g/min at the start of stimulation and $\Delta CMR_{Glc,ox}$ = 0.08 ± 0.04 μmol/g/min and $\Delta CMR_{O2}$ = 0.1 ± 0.05 μmol/g/min 12.8 min after the start of TGN stimulation. Data were averaged across the population of rats and are presented as Mean ± SEM.

calculated from the subtraction of time courses during stimulation and rest. For a more precise evaluation as a function of time, stimulated levels from 38.4 min to 64 min were subtracted from resting lactate levels from 32 min to 6.4 min. After 12.8 min of TGN stimulation, lactate changes were significantly reduced (0.73 ± 0.1 μmol/g to 0.2 ± 0.07 μmol/g, $p < 0.05$).

In an identical manner, Glu levels were increased 6.4 min after onset of stimulation (+11.6%, $p < 0.01$) and remained almost stable until the end of stimulation (Fig. 4B). Glu changes as function of time were calculated as for Lac changes. Although the baseline average Glu levels show some variation as a function of time (10.2 ± 0.9 μmol/g at 6.4 min vs 10.7 ± 0.9 μmol/g at 12.8 and 19.2 min, these were not significant ($p > 0.05$).

The estimates of $\Delta CMR_{Glc}$ and $\Delta CMR_{O2}$ from Lac and Glu changes rely on an oversimplified model of glucose oxidation proposed by Schaller et al. (2014). Since some assumptions may be debated, here three different methods were used to compare estimates. Method 1 calculated $\Delta CMR_{Glc}$ and $\Delta CMR_{O2}$ relative to rest levels. From Lac changes, $\Delta CMR_{Glc,non\text{-}ox}$ were evaluated (Fig. 4D). $\Delta CMR_{Glc,non\text{-}ox}$ dropped from 0.14 ± 0.05 μmol/g/min at the start of stimulation to 0.07 ± 0.03 μmol/g/min 12.8 min after the start of stimulation was observed (repeated measures ANOVA, $p = 0.01$). Glu changes were almost constant during 32 min (0.7 ± 0.08 μmol/g) (Fig. 4B). Since $\Delta CMR_{Glc,ox}$ and $\Delta CMR_{O2}$ calculations were proportional to ΔGlu, their evolution as a function of time demonstrated identical patterns, with $\Delta CMR_{Glc,ox}$ = 0.11 ± 0.06 μmol/g/min $\Delta CMR_{O2}$ = 0.13 ± 0.07 μmol/g/min at the start of stimulation and $\Delta CMR_{Glc,ox}$ = 0.08 ± 0.04 μmol/g/min and $\Delta CMR_{O2}$ = 0.1 ± 0.05 μmol/g/min 12.8 min after the start of TGN stimulation (Fig. 4D, E). Although not significant ($p > 0.05$), $\Delta CMR_{Glc,ox}$ and $\Delta CMR_{O2}$ decreased by 27% and 23% respectively at 12.8 min.

Instead of calculating changes in Glu relative to rest levels, changes were also calculated relative to each previous stimulation point during the course of stimulation (each time point during stimulation was subtracted from the next one-Method2). Using this scheme, changes in glutamate were significantly smaller at 12.8 min ($p < 0.05$) during stimulation and remained close to zero for the remaining stimulation period. $\Delta CMR_{Glc,ox}$ and $\Delta CMR_{O2}$ directly derived from these changes also demonstrated a decrease at 12.8 min post stimulation start and changes remained close to zero further dropping at the last time point during stimulation demonstrating negative values ($\Delta CMR_{Glc,ox}$ = 0.12 ± 0.07 μmol/g/min at the start of stimulation and $\Delta CMR_{Glc,ox}$ = -0.022 ± 0.04 μmol/g/min at 12.8 min during stimulation; $\Delta CMR_{O2}$ = 0.15 ± 0.08 μmol/g/min at the start of stimulation and $\Delta CMR_{O2}$ = −0.027 ± 0.04 μmol/g/min at 12.8 min during stimulation).

Both increases in Lac and Glu were accompanied by a decrease of Glc during stimulation levels (at rest:2.2 ± 0.11 μmol/g vs 1.3 ± 0.05 μmol/g during stimulation)

that was not significant due to large variability across animals (Fig. 4.C, Blue curve. 2 animals (out of 22) were removed from analysis as they showed increased Glc levels during stimulation. A significant decrease of Glc levels during TGN stimulation ($p = 0.03$) was then measured – Gray curve). Assuming that glucose transport is unchanged during stimulation, variations in glucose content can be employed to estimate the total $\Delta CMR_{Glc,tot}$ (Method3). In Fig. 4.D, changes in the rate of consumption of glucose calculated from either glucose measurements or glutamate and lactate (stimulation-rest) were compared showing that $\Delta CMR_{Glc,tot}$ estimates were comparable (0.29 ± 0.09 vs 0.22 ± 0.09 μmol/g/min, respectively, $p > 0.05$ repeated measures ANOVA). Interestingly, $\Delta CMR_{Glc,tot}$ calculated from Glu and Lac changes during the stimulation period only (Method2) had the same levels as $\Delta CMR_{Glc,tot}$ calculated from Glc levels (Method3) and as $\Delta CMR_{Glc,tot}$ calculated from Glu and Lac changes between stimulation and rest periods (Method1) at 6.4 min ($p > 0.05$ for $\Delta CMR_{Glc,tot\ (Method1)}$ versus $\Delta CMR_{Glc,tot\ (Method2)}$ versus $\Delta CMR_{Glc,tot\ (Method3)}$) but then decreased to identical changes in consumption rate of non-oxidative Glc (orange curve) until the end of the stimulation. Table 1 summarizes results obtained 6.4 min and 12.8 min after the start of stimulation for each method.

## DISCUSSION

In our previous studies, paradigms of stimulation were developed to minimize habituation effects in BOLD timecourses (Sonnay et al., 2015, 2016). Here, the 1minOFF-1minON... paradigm demonstrated significant changes in BOLD amplitudes although BOLD responses remained positive as a function of time and CBV changes appeared lessened as seen by low baseline drifts. However, recent studies showed that BOLD responses may not represent accurately the underlying physiological processes (Moradi and Buxton, 2013). Therefore, we investigated the effects of habituation processes on concentrations of metabolites involved in energy metabolism. Variations in the concentration of lactate, glucose and glutamate can be used to infer on $CMR_{glc}$ and $CMR_{O2}$ changes.

In a preceding work, we established the feasibility of investigating the metabolism of the barrel cortex during brain activation using fMRS (Just et al., 2013). Here, the quality of the proton spectra was further improved using the following means: spectra were acquired sequentially on 22 rats under carefully controlled physiology and the rat holder was tilted in the magnet (30 or 45°) allowing enlargement of the VOI in the barrel cortex of the rat (16 $mm^3$ to 22.5 $mm^3$) without partial volume effects compared to the previous study (Just et al., 2013). Operating in this way allowed obtaining reproducibly shimmed (water linewidth = 10 ± 2 Hz) spectra in S1BF from rat to rat ($SNR_{LCModel} = 26 \pm 4$, $n = 22$) as is usually the case for humans. At the same time, the temporal span of spectra acquisition was increased from 10 min to 32 min allowing more averaging as we showed it is possible to maintain activation of the somatosensory cortex of rats for up to 2 h (Sonnay et al., 2015).

In S1BF, absolute metabolite concentration changes during TGN stimulation were in agreement with our previous findings: +7.5% for [Glu] and −10.7% for [Glc] although results were smaller for [Asp] (−6.3% change in contrast to −24%) and for [Lac] (+109% instead of +198%), differences that we attribute to the increased length of the stimulation and hence more averaging across a longer time. On the other hand, the LCModel fitted BOLD-free difference spectrum allowed to find a 3% increase in [Glu] and a 27% increase in [Lac] during S1BF activation in closer agreement to findings in the human visual cortex (Schaller et al., 2014; Bednarík et al., 2015).

### Temporal analysis of barrel cortex metabolism during activation

The temporal analysis of metabolites during rest and stimulation yielded significant increases in both [Glu] and [Lac] six minutes after the start of TGN stimulation. Lactate levels were decreased during the remaining stimulation period. Simultaneously, a decrease in glucose levels was found at 6.4 min during stimulation and these levels remained low until the end of stimulation although variability was high across subjects. The direction (positive or negative) of these temporal changes matched with previous findings (Just et al., 2013). However, previous measurements were obtained over a 10-min period of continuous TGN stimulation as in humans (Mangia et al., 2007) with a higher temporal resolution where [Lac] remained at steady-state during 10 min of stimulation and [Glu] slowly increased to a maximum value around 6 min followed by a tendency to decrease as a function of time (Just et al., 2013) as was

**Table 1.** $\Delta CMR_{Glc,non\text{-}ox}$, $\Delta CMR_{Glc,ox}$, $\Delta CMR_{Glc,\ tot}$ and $\Delta CMR_{O2}$ values obtained at 6.4 min and 12.8 min using Lactate, Glutamate and Glucose timecourses (Fig. 4A–C). Calculations of $\Delta CMR_{Glc,non\text{-}ox}$, $\Delta CMR_{Glc,ox}$, $\Delta CMR_{Glc,\ tot}$ and $\Delta CMR_{O2}$ using a simplified model for Glucose metabolism were described by Schaller et al. (2014). In Method1, changes in Lactate and Glutamate as a function of time were calculated as the difference between Lactate or Glutamate concentrations during stimulation and rest at their respective time point. In Method2, changes in Lactate and Glutamate as a function of time were calculated as the difference between Lactate or Glutamate concentrations at a specific time point relative to Lactate or Glutamate concentrations at the previous time point. Method3 represents the calculation of $\Delta CMR_{Glc,\ tot}$ from glucose measurements (Fig. 4.C). Data were averaged across the population of rats and are presented as Data ± SEM

| | ΔCMRGlc,nonox 6.4 min | μmol/g/min 12.8 min | ΔCMRGlc,ox 6.4 min | μmol/g/min 12.8 min | ΔCMRGlc,tot 6.4 min | μmol/g/min 12.8 min | ΔCMRO2 6.4 min | μmol/g/min 12.8 min |
|---|---|---|---|---|---|---|---|---|
| Method1 | 0.14 ± 0.07 | 0.07 ± 0.03 | 0.11 ± 0.06 | 0.08 ± 0.04 | 0.29 ± 0.09 | 0.18 ± 0.05 | 0.13 ± 0.07 | 0.1 ± 0.05 |
| Method2 | 0.14 ± 0.05 | 0.004 ± 0.015 | 0.12 ± 0.07 | 0 | 0.29 ± 0.09 | 0 | 0.15 ± 0.08 | 0 |
| Method3 | N/A | N/A | N/A | N/A | 0.22 ± 0.09 | 0.17 ± 0.08 | N/A | N/A |

the case in the present study. With the lower temporal resolution used in the present study, it is possible that the maximum [Lac] change was reached at an earlier time point. In agreement with previous studies (Prichard et al., 1991; Frahm et al., 1996; Lin et al., 2012), we observed an increase in [Lac] followed by a decrease which was attributed to differences in the excited neuronal populations by Lin et al. (2012). However, the decline in lactate levels may also be attributed to habituation mechanisms, especially for prolonged stimulations (Vafaee et al., 2012) or to subsequent lactate diffusion out of the volume of interest and/or its utilization by brain cells (Duarte et al., 2015) that could further explain neuronal fine tuning.

### Estimates of $\Delta CMR_{Glc}$ and $\Delta CMR_{O2}$

Although during the past years there has been important work both at the measurement level and modeling level describing the relationship between oxidative energy and glutamatergic neurotransmission as summarized by Hyder and Rothman (2012), many studies have focused on the first few minutes only after the start of stimulation. To our knowledge the fate of glutamate neurotransmission as the task is prolonged has attracted less attention although several studies have described changes in BOLD, CBF, $CMR_{O2}$ during prolonged stimulation periods (Vafaee et al., 2012; Lin et al., 2009, Mintun et al., 2002). To date, several $^{1}$H-fMRS studies showed that glucose levels were significantly reduced during prolonged stimulations (Mangia et al., 2007; Schaller et al., 2013; Just et al., 2013). Nevertheless, these studies also demonstrated that both Glu and Lac increased and reached new steady-state levels lasting for the entire stimulation period meaning that Glu is continuously recycled. Therefore, we assumed the same model of ATP consumption as used at the start of stimulation (Schaller et al., 2014) to determine both $\Delta CMR_{Glc}$ and $\Delta CMR_{O2}$ as a function of stimulation time.

In the present study, changes in consumption rates of total glucose derived from [Glc] measurements as a function of time remained constant during prolonged TGN stimulation. Using the simplified model of glucose oxidation proposed by Schaller et al. (2014), $\Delta CMR_{Glc,tot}$ derived from the sum of $\Delta CMR_{Glc,\ nonox}$ and $\Delta CMR_{Glc,\ ox}$ calculated from the respective changes in [Lac] and [Glu] as a function of time matched findings with [Glc] measurements (Method3). Interestingly, $\Delta CMR_{O2}$ and $\Delta CMR_{Glc,ox}$ also remained constant during the entire stimulation period. However, at 12.8 min following the prolonged stimulation onset, $\Delta CMRGlc_{,nonox}$ declined. These reductions were verified with the different methods to calculate changes in Lactate and Glutamate and represented between 45 and 100% reduction in glucose consumption rates. Method 1 suggested that respective non-oxidative and oxidative glucose consumption rates were reduced due to habituation processes but adapted so that the total glucose consumption rate was maintained until the end of the stimulation. Potentially identical adaptation mechanisms exist for the consumption rate of oxygen during prolonged stimulation. In addition, the agreement found between Method 1 and Method 3 appeared to validate estimates of $\Delta CMR_{Glc,\ nonox}$, $\Delta CMR_{Glc,\ ox}$ and $\Delta CMR_{O2}$ using the model proposed by Schaller et al. (2014). Method 2 was used as changes in Glu and Lac during prolonged activation of the rat barrel cortex seemed a more appropriate account of the ongoing physiology of the region of interest than in Method 1. Using Method 2, changes in consumption rates of glucose and oxygen were considered null 12.8 min after the start of stimulation suggesting that in this case $CMR_{Glc}$ and $CMR_{O2}$ remained at the values estimated at 6.4minutes post-onset during the remaining stimulation period. Interestingly, after 6.4 min of stimulation, changes in consumption rates of total glucose estimated with Method 2 matched almost exactly changes in consumption rates of non-oxidative glucose estimated from lactate changes as a function of time. The model proposed by Schaller et al. (2014) assumes that Lactate reflects only non-oxidative metabolism whereas Lactate release may also result from oxidative metabolism (Boumezbeur et al., 2010). Method 2 suggested that Lac changes during TGN stimulation were not providing sufficient energy (from non-oxidative or oxidative metabolism) for sustaining glucose consumption during the entire prolonged stimulation period given the mismatch between estimated and measured rates of total glucose consumption. Altogether, our results indicate that early S1BF BOLD activation is mediated by an increased non-oxidative glucose metabolism associated with lactate production as well as an increased oxidative glucose metabolism. As lactate release decreased during prolonged S1BF stimulation in line with earlier previous observations (Frahm et al., 1996; Hyder et al., 1997) but glutamate levels remained almost constant, the present study supports prevalence of oxidative metabolism during extended activation of the rat barrel cortex in accordance with previous studies in rats (Hyder et al., 1996) as well as in humans (Schaller et al., 2014). Nonetheless, $\Delta CMR_{Glc,\ ox}$ values calculated from glutamate increases after stimulation onset were significantly smaller (0.12–0.13 μmol/g/min) compared to previous values found by Hyder et al. (1996) (0.37–0.49 μmol/g/min) during sustained one-hour forepaw stimulation. These rates were compared using the same calculations with rates obtained during 10 min-continuous stimulations of the barrel cortex obtained in a previous study (Just et al., 2013). Prevalence of oxidative glucose metabolism during S1BF stimulation with the following rates $\Delta CMR_{Glc,non\text{-}ox,cont}$ = 0.061 μmol/g/min, $\Delta CMR_{Glc,ox,cont}$ = 0.17 μmol/g/min and $\Delta CMR_{O2}$ = 0.21 μmol/g/min was also obtained. $\Delta CMR_{O2}$ were also substantially smaller compared to findings by Hyder et al.(1996) (0.13–0.15 μmol/g/min versus 2.78–2.97 μmol/g/min). $\Delta CMR_{Glc,\ tot}$ values estimated from glucose measurements were also significantly lower compared to values reported by Ueki et al. (1988) while values estimated with Method 1 and 2 were comparable to lower limit values reported in the same study (Ueki et al.1988; Dienel, 2012) and with those reported by Nakao et al.(2001). Habituation led to a small but non-significant decline of mean changes in oxidative glucose consumption (0.13 ± 0.06 versus 0.09 ± 0.04 μmol/g/min representing a $CMR_{Glc,ox}$ change of 25% versus 35% during the first few minutes of stimulation assuming

$CMR_{Glc,rest}$ = 0.39 μmol/g/min (Nakao et al.,2001) while oxygenation consumption rates were almost identical. Assuming a resting $CMR_{O2}$ of 1.51 μmol/g/min (Hyder et al.,1996), the range of relative $\Delta CMR_{O2}$ increase for the present study was 9–10% 6.4 min after onset of stimulation and only 6–7% after 12.8 min of stimulation. Using 13C-fMRS during infusion of glucose and 4-h forepaw stimulation with a repeated 10sON-30sOFF-10sON paradigm of stimulation of the rat forepaw under α-chloralose, we also found a $\Delta CMR_{Glc,ox}$ = 0.067 μmol/g/min representing an increase of only 15% compared to baseline levels (Sonnay et al., 2016). The magnitude of changes was in agreement with our present findings. On the other hand, in Sonnay et al., 2016, we found $\Delta CMR_{O2}$ = 0.45 - μmol/g/min due to stimulation representing a 16% increase approximately ($CMR_{O2}$ (rest) = 2.84 μmol/g/min) indicating that our methodology may underestimate oxygenation consumption rates as expected from the assumptions of the model used. Nevertheless, smaller findings in the present study may be attributable to the 1minON-1minOFF paradigm used in the present study demonstrating a smaller BOLD decay rate ($\tau^{-1}$ = 0.2%/min; Fig. 1.F) compared to a continuous paradigm ($\tau^{-1}$ = 1.4%/min; Fig. 1.F) requiring higher levels of glucose and oxygen for stimulation which would explain discrepancies between present findings and values obtained by Hyder et al. (1996).

With Positron Emission Tomography (PET), Vafaee et al. (2012) reported that oxygen consumption declined significantly due to habituation mechanisms (upon extension of finger-tapping up to 20 min), in the human somatosensory cortex before recovering to initial resting levels. Lin et al. (2009) on the other hand, reported constant changes in $CMR_{O2}$ up to 6 min of stimulation with a subsequent increase of $CMR_{O2}$ up to 25 min of visual stimulation in the human brain that authors deemed necessary for stimulation to continue and explained by an increase in oxidative metabolism. These changes were concomitant with a decrease of the magnitude of BOLD responses after 21 min of stimulation while CBF changes also strongly declined. By contrast, CBF increased and remained constant during 20 min of stimulation in the study performed by Vafaee et al. (2012). CBF increases in the range 66–165% during continuous forepaw stimulation in rats under α-chloralose anesthesia were reported by Hyder et al. (1996) and only 17% (28% $CMR_{Glc}$ increase) for vibrissal stimulation under α-chloralose anesthesia by Nakao et al. (2001). The physiological analysis of data in Hyder et al. (1996) was consistent with a positive BOLD response during sustained stimulation. After 30 min of TGN stimulation, positive BOLD responses were still present in our study. However, Hyder et al.'s BOLD data did not show signs of habituation processes unlike in the present study. On the contrary, Silva et al. (1999) reported a 37% CBF decrease concomitant with a 30% BOLD decrease during a second period of forepaw stimulation lasting 30 s after one minute rest compared to a first period of forepaw stimulation in closer agreement with our findings. These results suggest that CBF increases may also have been attenuated during the course of prolonged TGN stimulation. Although measurements of CBF changes under identical conditions would be needed to validate our hypothesis, our results were closer to those reported by Lin et al.(2009) as changes in the consumption rate of oxygen were smaller as a function of time but remained positive until the end of the stimulation suggesting increased $CMR_{O2}$ levels together with increased $CMR_{Glc}$ compared to the rest period.

Other studies (Griffeth and Buxton, 2011; Moradi et al., 2012; Moradi and Buxton, 2013) were able to define changing coupling patterns between CBF and $CMR_{O2}$ and showed that BOLD responses did not reflect the underlying physiology (Buxton et al., 2014). Here, the amplitude of BOLD responses significantly decayed as a function of time due to habituation/adaptation processes but the amplitude of this decay was largely overestimated compared to changes in $CMR_{O2}$ or $CMR_{Glc}$. Non-oxidative, oxidative glucose and oxygen metabolisms adapted so that the total glucose consumption rate and the consumption rate of oxygen remained constant to sustain TGN stimulation. Nevertheless, only non-oxidative metabolism demonstrated significant changes during prolonged stimulation similarly to BOLD effects. In the present paper, we attribute this phenomenon to habituation mechanisms leading to adaptation mechanisms involving lactate diffusion out of the volume of interest as well as increased consumption of Lac by specific cells (Aubert et al., 2005). As a result of this, fine tuning mechanisms would emerge. Validation of these possibilities will indeed be required. Using the simplified model proposed by Schaller et al. (2014), prevalence of oxidative metabolism during prolonged TGN stimulation was confirmed using different methods thereby also validating usage of the simplified model.

In conclusion, our fMRI-fMRS study shows that although BOLD responses to a repeated stimulation paradigm decrease as a function of time due to mild habituation/adaptation processes, the global energetic status of the activated area under investigation was maintained during prolonged stimulation. Findings suggested potential adaptation of glycolytic metabolism as lactate decreased during ongoing TGN stimulation similarly to BOLD effect while glutamate and glucose remained stable. This study further suggested that the magnitude of BOLD changes does not reflect the underlying physiological processes under specific conditions such as adaption. However, BOLD decay rates may be evaluated and indicative of the strength of habituation/adaptation effects. In the present paper, issues related to the shape of the BOLD responses were not addressed. BOLD responses were estimated using a gamma-variate function that may not be representative of the rat's hemodynamic response (Amirmohseni et al., 2016). These may have an impact on the correct estimation of BOLD responses. We are currently investigating this impact with high resolution methodologies such as line scanning (Albers et al., 2016). A better estimate of BOLD responses could certainly improve estimates of consumption rates of oxygen and effects of habituation. Further investigations with stronger habituation effects will be necessary as well as

CBF measurements for a better characterization of neurovascular coupling mechanisms using proton functional MR spectroscopy.

*Acknowledgments—We thank Dr Carola Jaquelina Romero for technical assistance with animals. This study was supported by the Centre d'Imagerie BioMédicale (CIBM) of Ecole Polytechnique Fédérale de Lausanne (EPFL), the University of Lausanne (UNIL), the Foundations Leenards et Jeantet and a National Competence Center Biomedical Imaging (NCCBI) grant to Drs Joao MN Duarte and Nathalie Just.*

## REFERENCES

Adibi M, McDonald JS, Clifford CWG, Arabzadeh E (2013) Adaptation improves neural coding efficiency despite increasing correlations in variability. J Neurosci 33:2108–2120.

Albers, Franziska Schmid, Florian Wachsmuth, Lydia Faber, Cornelius (2016). Line scanning BOLD FMRI upon optogenetic stimulation, In: Proceedings of 24th meeting of the International Society of Magnetic Resonance in Medicine, Singapore, 488.

Amirmohseni S, Segelcke D, Reichl S, Wachsmuth L, Görlich D, Faber C, Pogatzki-Zahn E (2016) Characterization of incisional and inflammatory pain in rats using functional tools of MRI. Neuroimage 27:110–122. http://dx.doi.org/10.1016/j.neuroimage.2015.11.052.

Attwell D, Iadecola C (2002) The neurol basis of functional brainimaging signals. Trends Neurosci 25:621–625.

Aubert A, Costalat R (2002) A model of the coupling between brain electrical activity, metabolism, and hemodynamics: application to the interpretation of functional neuroimaging. Neuroimage 17 (3):1162–1181.

Aubert A, Costalat R, Magistretti PJ, Pellerin L (2005) Brain lactate kinetics: modeling evidence for neuronal lactate uptake upon activation. Proc Natl Acad Sci U S A 102(45):16448–16453.

Bednařík P, Tkáč I, Giove F, DiNuzzo M, Deelchand DK, Emir UE, Eberly LE, Mangia S (2015) Neurochemical and BOLD responses during neuronal activation measured in the human visual cortex at 7 Tesla. J Cereb Blood Flow Metab 35:601–610. http://dx.doi.org/10.1038/jcbfm.2014.233.

Boumezbeur F, Petersen KF, Cline GW, Mason GF, Behar KL, Shulman GI, Rothman DL (2010) The contribution of blood lactate to brain energy metabolism in humans measured by dynamic $^{13}C$ nuclear magnetic resonance spectroscopy. J Neurosci 30:13983–13991.

Buxton RB, Uludağ K, Dubowitz DJ, Liu TT (2004) Modeling the hemodynamic response to brain activation. Neuroimage 23(Suppl 1):S220–S233.

Buxton RB, Griffeth VE, Simon AB, Moradi F, Shmuel A (2014) Variability of the coupling of blood flow and oxygen metabolism responses in the brain: a problem for interpreting BOLD studies but potentially a new window on the underlying neural activity. Front Neurosci 11(8):139. http://dx.doi.org/10.3389/fnins.2014.00139.

Dienel GA (2012) Brain lactate metabolism: the discoveries and the controversies. J Cereb Blood Flow Metab 32(7):1107–1138.

Duarte JM, Girault FM, Gruetter R (2015) Brain energy metabolism measured by (13)C magnetic resonance spectroscopy in vivo upon infusion of [3-(13)C]lactate. J Neurosci Res 93 (7):1009–1018. http://dx.doi.org/10.1002/jnr.23531.

Enager P, Piilgaard H, Offenhauser N, Kocharyan A, Fernandes P, Hamel E, Lauritzen M (2009) Pathway-specific variations in neurovascular and neurometabolic coupling in rat primary somatosensory cortex. J Cereb Blood Flow Metab 29 (5):976–986. http://dx.doi.org/10.1038/jcbfm.2009.23.

Frahm J, Krüger G, Merboldt KD, Kleinschmidt A (1996) Dynamic uncoupling and recoupling of perfusion and oxidative metabolism during focal brain activation in man. Magn Reson Med 35 (2):143–148.

Friston KJ, Holmes AP, Poline JB, Grasby PJ, Williams SC, Frackowiak RS, Turner R (1995) Analysis of fMRI time-series revisited. Neuroimage 2(1):45–53.

Griffeth VE, Buxton RB (2011) A theoretical framework for estimating cerebral oxygen metabolism changes using the calibrated-BOLD method: modeling the effects of blood volume distribution, hematocrit, oxygen extraction fraction, and tissue signal properties on the BOLD signal. Neuroimage 58(1):198–212. http://dx.doi.org/10.1016/j.neuroimage.2011.05.077.

Gruetter R, Tkác I (2000) Field mapping without reference scan using asymmetric echo-planar techniques. Magn Reson Med 43:319–323.

Hyder F, Chase JR, Behar KL, Mason GF, Siddeek M, Rothman DL, Shulman RG (1996) Increased tricarboxylic acid cycle flux in rat brain during forepaw stimulation detected with 1H[13C]NMR. Proc Natl Acad Sci U S A 93(15):7612–7617.

Hyder F, Kida I, Behar KL, Kennan RP, Maciejewski PK, Rothman DL (2001) Quantitative functional imaging of the brain: towards mapping neuronal activity by BOLD fMRI. NMR Biomed 14(7–8): 413–431.

Hyder F, Rothman DL, Mason GF, Rangarajan A, Behar KL, Shulman RG (1997) Oxidative glucose metabolism in rat brain during single forepaw stimulation: a spatially localized 1H[13C] nuclear magnetic resonance study. J Cereb Blood Flow Metab 17 (10):1040–1047.

Hyder F, Rothman DL (2012) Quantitative fMRI and oxidative neuroenergetics. Neuroimage 62(2):985–994. http://dx.doi.org/10.1016/j.neuroimage.2012.04.027.

Just N, Petersen C, Gruetter R (2010) BOLD responses to trigeminal nerve stimulation. Magn Reson Imaging. 28(8):1143–1151. http://dx.doi.org/10.1016/j.mri.2010.02.002.

Just N, Xin L, Frenkel H, et al. (2013) Characterization of sustained BOLD activation in the rat barrel cortex and neurochemical consequences. Neuroimage 74:343–351.

Larsson J, Solomon SG, Kohn A (2015) FMRI adaptation revisited. Cortex. pii: S0010-9452(15)00379-2. doi: 10.1016/j.cortex.2015.10.026.

Lin AL, Fox PT, Yang Y, Lu H, Tan LH, Gao JH (2009) Time-dependent correlation of cerebral blood flow with oxygen metabolism in activated human visual cortex as measured by fMRI. Neuroimage 44:16–22.

Lin Y, Stephenson MC, Xin L, Napolitano A, Morris PG (2012) Investigating the metabolic changes due to visual stimulation using functional proton magnetic resonance spectroscopy at 7 T. J Cereb Blood Flow Metab 32(8):1484–1495.

Mangia S, Tkác I, Gruetter R, Van de Moortele PF, Maraviglia B, Uğurbil K (2007) Sustained neuronal activation raises oxidative metabolism to a new steady-state level: evidence from 1H NMR spectroscopy in the human visual cortex. J Cereb Blood Flow Metab 27(5):1055–1063.

Maravall M, Petersen RS, Fairhall AL, Arabzadeh E, Diamond ME (2007) Shifts in coding properties and maintenance of information transmission during adaptation in barrel cortex. PLoS Biol 5:e19.

Mlynarik V, Gambarota G, Frenkel H, et al. (2006) Localized short-echo-time proton MR spectroscopy with full signal-intensity acquisition. Magn Reson Med 56:965–970.

Moradi F, Buračas GT, Buxton RB (2012) Attention strongly increases oxygen metabolic response to stimulus in primary visual cortex. Neuroimage 59(1):601–607. http://dx.doi.org/10.1016/j.neuroimage.2011.07.078.

Moradi F, Buxton RB (2013) Adaptation of cerebral oxygen metabolism and blood flow and modulation of neurovascular coupling with prolonged stimulation in human visual cortex. Neuroimage 82:182–189. http://dx.doi.org/10.1016/j.neuroimage.2013.05.110.

Mintun MA, Vlassenko AG, Shulman GL, Snyder AZ (2002) Time-related increase of oxygen utilization in continuously activated human visual cortex. Neuroimage 16(2):531–537.

Musall S, von der Behrens W, Mayrhofer JM, Weber B, Helmchen F, Haiss F (2014) Tactile frequency discrimination is enhanced by circumventing neocortical adaptation. Nat Neurosci 17 (11):1567–1573. http://dx.doi.org/10.1038/nn.3821.

Nakao Y, Itoh Y, Kuang TY, Cook M, Jehle J, Sokoloff L (2001) Effects of anesthesia on functional activation of cerebral blood flow and metabolism. Proc Natl Acad Sci U S A 98 (13):7593–7598.

Prichard J, Rothman D, Novotny E, Petroff O, Kuwabara T, Avison M, Howseman A, Hanstock C, Shulman R (1991) Lactate rise detected by 1H NMR in human visual cortex during physiologic stimulation. Proc Natl Acad Sci U S A 88(13):5829–5831.

Schaller B, Mekle R, Xin L, Kunz N, Gruetter R (2013) Net increase of lactate and glutamate concentration in activated human visual cortex detected with magnetic resonance spectroscopy at 7 tesla. J Neurosci Res 91(8):1076–1083. http://dx.doi.org/10.1002/jnr.23194.

Schaller B, Xin L, O'Brien K, Magill AW, Gruetter R (2014) Are glutamate and lactate increases ubiquitous to physiological activation? A (1)H functional MR spectroscopy study during motor activation in human brain at 7Tesla. Neuroimage 93(Pt 1):138–145. http://dx.doi.org/10.1016/j.neuroimage.2014.02.016.

Silva AC, Lee SP, Yang G, Iadecola C, Kim SG (1999) Simultaneous blood oxygenation level-dependent and cerebral blood flow functional magnetic resonance imaging during forepaw stimulation in the rat. J Cereb Blood Flow Metab 19(8):871–879.

Sonnay S, Just N, Duarte JM, Gruetter R (2015) Imaging of prolonged BOLD response in the somatosensory cortex of the rat. NMR Biomed 28(3):414–421. http://dx.doi.org/10.1002/nbm.3263.

Sonnay S, Duarte JM, Just N, Gruetter R (2016) Compartmentalised energy metabolism supporting glutamatergic neurotransmission in response to increased activity in the rat cerebral cortex: A 13C MRS study in vivo at 14.1 T. J Cereb Blood Flow Metab 36 (5):928–940. http://dx.doi.org/10.1177/0271678X16629482.

Vafaee MS, Vang K, Bergersen LH, Gjedde A (2012) Oxygen consumption and blood flow coupling in human motor cortex during intense finger tapping: implication for a role of lactate. J Cereb Blood Flow Metab 32(10):1859–1868. http://dx.doi.org/10.1038/jcbfm.2012.89.

Ueki M, Linn F, Hossman KA (1988) Functional activation of cerebral blood flow and metabolism before and after global ischemia of rat brain. J Cereb Blood Flow Metab 8:486–494.

*(Received 12 September 2016, Accepted 23 January 2017)*
*(Available online 30 January 2017)*